Diffusion in Ion-Exchanged Clinoptilolites

Mark W. Ackley and Ralph T. Yang
Dept. of Chemical Engineering, State University of New York, Buffalo, NY 14260

The two-dimensional channel structure of clinoptilolite has been altered systematically by ion exchange to study the effects of cation type, size, location, and distribution on the diffusion of N_2 and CH_4 probe molecules. Concentration-dependent diffusion time constants (D/L^2) were determined from gravimetric uptake measurements for fully-exchanged K^+, Na^+, and H^+ clinoptilolites, and highly-exchanged Ca^{2+} (89%) and Mg^{2+} (72%) clinoptilolites. Both plane sheet and parallel channel diffusion models were developed from the one-dimensional plane sheet diffusion equation and fit to the uptake data. Resulting values of D/L^2 varied by a factor of more than 1,000 for both N_2 and CH_4, while kinetic selectivity spanned nearly two orders of magnitude for this group of modified clinoptilolites. Achieving this range in performance for the difficult N_2/CH_4 separation demonstrates the excellent potential for tailoring clinoptilolite by cation manipulation for the kinetic separation of other gas mixtures.

Introduction

Interest in upgrading aging natural gas wells by noncryogenic means continues to fuel research of the difficult problem of separating nitrogen/methane mixtures. Ackley and Yang (1990) have demonstrated the use of carbon molecular sieve (CMS) for kinetic separation of N_2/CH_4 mixtures in pressure swing adsorption (PSA) processes, but have also shown that the potential for CMS to achieve the desired pipeline quality (90% methane) is doubtful. The PSA-type process demonstrated by Habgood (1958a) using 4A molecular sieve for this separation achieved desirable results at very limiting conditions (273 K, CH_4 feed $\geq$ 90%). Although separation can often be improved through process optimization, maximum performance is limited by the adsorption characteristics of the sorbent. More promising separation of N_2/CH_4 mixtures was achieved by PSA using calcium-exchanged clinoptilolite (Frankiewicz and Donnelly, 1983).

A review of the literature revealed very little information concerning the diffusion of gases and vapors in clinoptilolites. Ma and Lee (1978) measured sorption rates and diffusivities of SO_2 in two natural clinoptilolites, and Torii et al. (1975) measured the uptake rates of CO_2, CH_4, C_2H_6, N_2, and C_3H_8 on several partially-exchanged clinoptilolites. Frankiewicz and Donnelly (1983) measured both pure and mixed gas diffusion coefficients for N_2 and CH_4 on one raw natural clinoptilolite and its partially-exchanged (Ca^{2+}) derivative.

Zeolites can be tailored through ion exchange to affect desired gas separations by exploiting equilibrium and/or kinetic properties. The success of such tailoring, however, depends largely on the interrelation between the zeolite structure and the gas adsorption/diffusion characteristics. The mixture of cations contained in natural clinoptilolites, as well as in most exchanged clinoptilolites described in the literature, complicates the understanding of this relationship. An intent of this research was to produce fully-exchanged clinoptilolites, each containing a single cation type. The gases CH_4 (nonpolar) and N_2 (small quadrupole moment) served as probe molecules of similar kinetic diameter, but different shape. Both adsorption (Ackley and Yang, 1991) and diffusion of these gases in modified clinoptilolites were measured. This article addresses the diffusion characteristics only.

Fully-exchanged clinoptilolite sorbents were achieved for the monovalent cations K^+, Na^+, and H^+, while highly-exchanged (89% and 72%) materials resulted for the bivalent cations Ca^{2+} and Mg^{2+}, respectively. A purified form of the raw natural zeolite was also included in the study. Gravimetric, differential uptakes were measured at 300 K and 323 K for N_2/He and CH_4/He mixtures. A parallel channel diffusion model was derived using the 1-D (one-dimensional) plane sheet diffusion equation to represent the rapid and slow components of diffusion evident from the uptake rate data. This allowed the determination of the concentration-dependent diffusion time constants $(D/L^2)_i$ for both the eight- and ten-member ring channels of the clinoptilolite structure. Diffusion time con-

Current address of M. W. Ackley: Union Carbide Industrial Gases Inc., Linde Div., P.O. Box 44, Tonawanda, NY 14151.

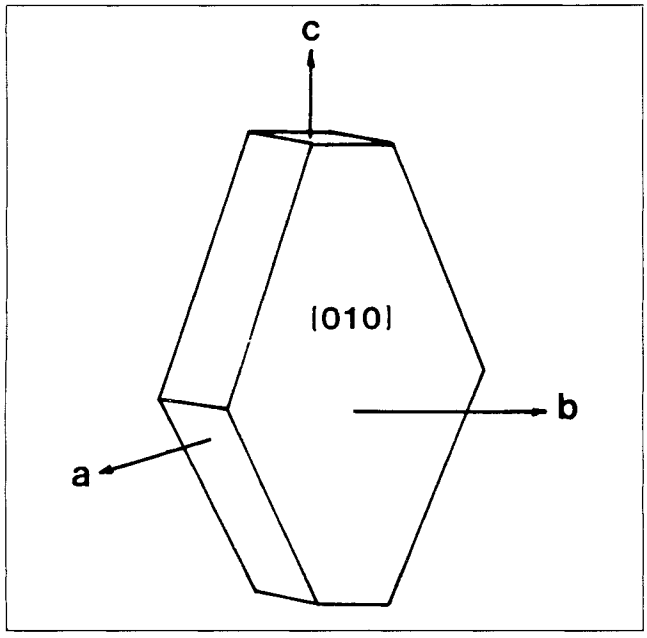

Figure 1. Clinoptilolite unit cell coordinate system relative to a single crystal.

stants varied by more than three orders of magnitude, and kinetic selectivities spanned more than two orders of magnitude for this group of modified clinoptilolites. The kinetic separation of N_2/CH_4 has been discussed in terms of channel blockage as related to the type, size, location and distribution of cations.

Structure of Clinoptilolite

Framework

Clinoptilolite is the most abundant of the natural zeolites (Mumpton and Ormsby, 1976), but composition and purity vary widely among the many deposits found throughout the world. Clinoptilolite has been successfully synthesized only on a very small scale (Goto, 1977; Chi and Sand, 1983), thus inhibiting fundamental studies of the pure, single-cation species of this mineral.

A member of the Heulandite Group of natural zeolites, clinoptilolite is isostructural with the zeolite Heulandite. The general formula for natural zeolites is:

$$(\mathrm{Li, Na, K})_a(\mathrm{Mg, Ca, Sr, Ba})_d[\mathrm{Al}_{(a+2d)}\mathrm{Si}_{n-(a+2d)}\mathrm{O}_{2n}]\cdot m\mathrm{H_2O}$$

The unit cell of clinoptilolite is monoclinic and is usually characterized on the basis of 72 O atoms ($n=36$) and $m=24$ water molecules, with Na^+, K^+, Ca^{2+}, and Mg^{2+} as the most common charge-balancing cations. Representative unit cell parameters for the $(Na, K)_6$ $(Al_6$ Si_{30} $O_{72})\cdot 20$ H_2O form are: $a=1.762$ nm, $b=1.791$ nm, $c=0.739$ nm, $\beta=2.029$ rad (Gottardi and Galli, 1985). The corresponding unit cell volume is 2.091 nm^3. The coordinate system of the unit cell is shown relative to a single crystal in Figure 1. Scanning electron photomicrographs indicate that well-defined crystals span a size range [in the *a-c* plane (010) of the unit cell] from a few tenths of microns to several microns (Ackley and Yang, 1991). This classic crystalline morphology is evident only in small cavities that appear randomly in the raw material, however, while a majority of the clinoptilolite is anhedral characterized by densely packed platelets. The difficulty in synthesizing single crystals makes it virtually impossible to prepare a clinoptilolite sample of uniform crystalline size for adsorption studies. Characterization by a "crystalline" size distribution is not physically meaningful in view of the diverse morphology of the natural material.

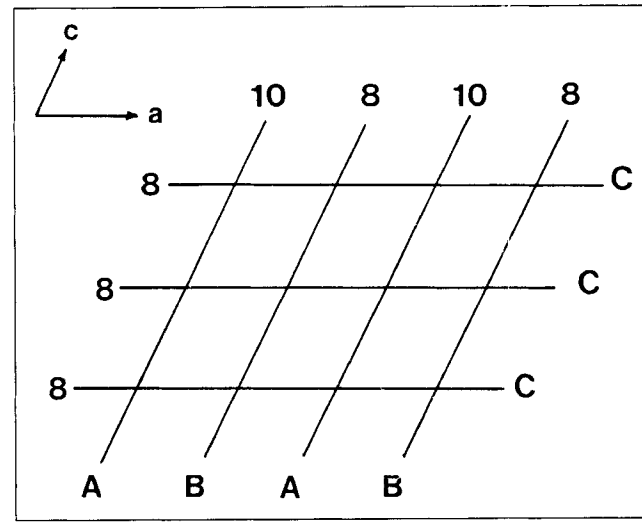

Figure 2. Orientation of clinoptilolite channel axes.

X-ray diffraction measurements were obtained for the purified and all ion-exchanged clinoptilolites (Ackley, 1991; Ackley et al., 1991). These results were used to determine unit cell parameters and to confirm the high degree of crystallinity in all samples.

Gas penetrates the clinoptilolite structure through a series of intersecting channels along the *a* and *c* axes, each layer of channels separated by a dense gas-impermeable layer of tetrahedral framework: that is, gas cannot move along the *b* axis. This 2-D microporous channel system was first characterized for Heulandite—the orientation of the channel axes in the *a-c* plane is illustrated in Figure 2 (Merkle and Slaughter, 1968). Gottardi and Galli (1985) provide an illuminating description of the topology of the tetrahedral frameworks of natural zeolites using the tetrahedra node/oxygen bridge convention. Using this description of the 4-4-1-1 heulandite unit, a model of the clinoptilolite framework was constructed. The 2-D channel system is apparent in the model as depicted in Figures 3a and 3b. Channels A (ten-member ring) and B (eight-member ring) are parallel to each other and the *c* axis of the unit cell, while the C channel (eight-member ring) lies along the *a* axis intersecting both A and B channels. A unit cell consists of portions of two A and B channel pairs—each pair located between adjacent framework layers. If projected into the *a-b* plane, this unit cell would extend to a depth defined by the width of the C channel. The crystalline framework structure is completely described in terms of its unit cell and open channel system in Figures 1 to 3. Charge-balancing cations have not been shown in these figures.

Cation sites

The selectivity and rate of uptake of gases are heavily in-

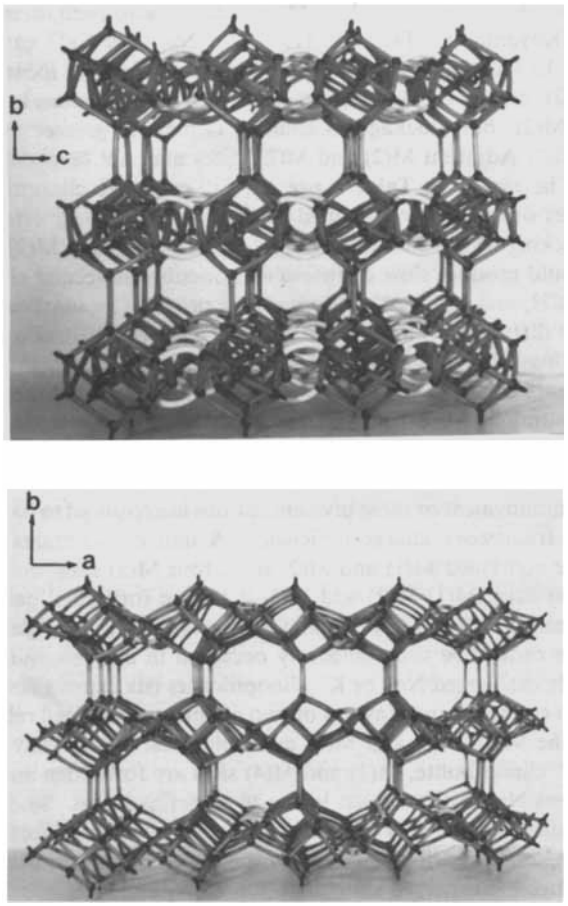

Figure 3. Model for framework structure of clinoptilolite.

fluenced by the type, number and location of the charge-balancing cations residing in the A, B, and C channels. Two notable refinements of the clinoptilolite structure provide cation site information (Alberti, 1975; Koyama and Takeuchi, 1977). The adsorption and diffusion characteristics determined from the present research have been related to the latter of these two studies since sites for all four of the naturally occurring, exchangeable cations (K^+, Na^+, Ca^{2+}, Mg^{2+}) have been determined. Definition of cation and water location and coordination within the clinoptilolite structure, however, is by no means complete.

Cation sites M(1)-M(4) are summarized in Table 1 relative to the channel system described above (Koyama and Takeuchi, 1977). The elliptic-shaped eight- and ten-member rings that form the channel system are nonplanar and cannot be simply dimensioned. Plane projections of these channels dimensioned in several studies (Barrer et al., 1967; Barrer, 1982; Breck, 1974) all relate to the original heulandite structure (Merkle and Slaughter, 1968). The approximate channel dimensions of Barrer (1982) and Breck (1974) given in Table 1 are used in this study. The Pauling ionic crystal radii of the five relevant exchangeable cations are given in Table 2 (Nightengale, 1959).

The critical diameter of the oxygen atom in the tetrahedra structure is 0.28 nm (Barrer, 1982). The collision diameters for N_2 and CH_4 are 0.364 nm and 0.38 nm, respectively. A

Table 1. Channel Characteristics and Cation Sites in Clinoptilolite

Channel	Tetrahedral Ring Size/ Channel Axis	Cation Site	Major Cations	Approx. Channel Dimensions nm × nm
A	10/*c*	M(1)	Na,Ca	0.72×0.44
B	8/*c*	M(2)	Ca,Na	0.47×0.41
C	8/*a*	M(3)	K	0.55×0.40
A	10/*c*	M(4)	Mg	0.72×0.44

Table 2. Exchangeable Cation Radii

Cation	Pauling Ionic Radius nm
Na^+	0.095
K^+	0.133
NH_4^+	0.148
Mg^{2+}	0.065
Ca^{2+}	0.099

smaller critical dimension of the linear N_2 molecule (0.30 nm) becomes relevant in diffusion if the N_2 major axis becomes aligned along a channel axis.

Using the information described above, the various cations (except NH_4^+) can be positioned within the channel system, and the degree of blockage can be estimated geometrically by considering the relative sizes of the channels, cations and diffusing molecules. Cross-sections of the A, B, and C channels with resident cations in the corresponding M(1)/M(2), M(3), and M(4) sites are illustrated in Figure 4. The C channel, eight-

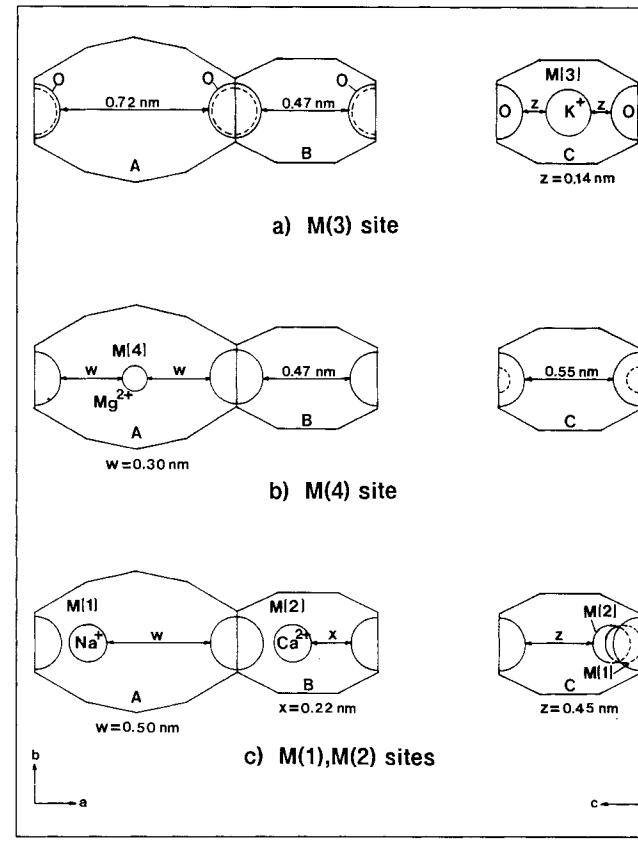

Figure 4. Channel blockage diagrams.

Table 3. Channel Blockage Matrix for Clinoptilolite

	Channel A		Channel B		Channel C	
Site	CH_4	N_2	CH_4	N_2	CH_4	N_2
M(1)/M(2)	pb	pb	b	b	pb	pb
M(3)	o	o	o	o	b	b
M(4)	b	pb	o	o	o	o

b = blocked; pb = partially blocked; o = open

member ring projections in this figure are taken at the joining interface of the A and B channels. This relationship between the different ring structure of the three channels is also demonstrated in Figure 3 where it is evident that each oxygen bridge atom separating the dense tetrahedra layers (represented by the vertical linear connectors in the model) is an edge member shared by all three rings.

The procedure used to estimate blockage considers only the lateral channel dimensions as described in the following example. Koyama and Takeuchi (1977) have located the K^+ cation at the M(3) site, that is, at the center of the eight-member ring that forms the C channel. Based on the width of this channel (0.55 nm) given in Table 1, it is evident that the opening is restricted to approximately 0.14 nm resulting in total blockage to the transfer of either CH_4 or N_2 molecules. The eight-member ring of the C channel is also the interface between the A and B channels. The O-atoms shown in Figure 4a (the bridge atoms between the dense tetrahedra layers) overshadow the K^+ cations in their projections into the *a-b* plane such that the O-atoms remain the dominant restrictions to diffusion into these channels. This rationalization leads immediately to a one-dimensional independent diffusion in channels A and B with no diffusion through channel C by the full exchange of K^+ in clinoptilolite. This structure is the basis for the 1-D diffusion model described below.

By applying the above reasoning to the M(4) and M(1)/M(2) sites and considering the full exchange of Ca^{2+}, Na^+, and Mg^{2+} cations, a channel blockage matrix has been devised in Table 3. Since Ca^{2+} and Na^+ may occupy both M(1) and M(2) sites, pore blockage has been determined considering the combined occupancy of these sites. M(1) and M(2) sites are located at the channel intersections and are not coordinated in either the eight- or ten-member rings. The intersecting channel regions may be slightly larger than the one suggested by the ring structures shown in Figure 4. A M(2)′ site has also been identified by Koyama and Takeuchi (1977) for Na^+ and Ca^{2+} cations, but its location is not shown in Figure 4. A cation located at M(2)′ creates the same blockage to the B channel as one located at M(2), but blockage to channel C may be greater due to M(2)′. Adjacent M(2) and M(2)′ sites may not be occupied.

The results in Table 3 present full-exchange clinoptilolite cases of interest for detailed diffusion studies: very effective blocking of the structure by Na^+ or Ca^{2+} in M(1)/M(2) sites should produce slow diffusion and possibly molecular sieving of CH_4 and N_2; the K^+-clinoptilolite provides an ideal case of 1-D diffusion with the possibility of different diffusion rates distinguishing the independent A and B channels; Mg^{2+} represents complete blockage of the ten-member ring A channel resulting in 2-D diffusion from eight-member ring channels B and C.

In an ideal clinoptilolite containing six Al^{3+} per unit cell, six monovalent or three bivalent cations are required to balance the framework charge deficiency. A unit cell contains only four combined M(1) and M(2) sites, four M(3) sites, and two M(4) sites. M(1)-M(3) and M(1)-M(4) are forbidden pairs of atomic positions (Koyama and Takeuchi, 1977): these pairs of sites cannot be simultaneously occupied in a given unit cell. Fully exchanged Na^+ or K^+ clinoptilolites (six cations per unit cell) can result in an excess of two cations per unit cell relative to the M(1)/M(2) and M(3) available sites, respectively. For Na^+ clinoptilolite, M(3) and M(4) sites are forbidden and the excess Na^+ cations must locate in undefined sites. Since the channels are already effectively blocked, anything short of a complete redistribution of all of the Na^+ cations is unlikely to change the expected slow diffusion of N_2 and CH_4.

The situation is more interesting for K^+ clinoptilolite. The excess K^+ cations could possibly locate in M(2) or M(4) sites, but Koyama and Takeuchi (1977) suggest the M(2) site location after filling of the M(3) sites. Figure 4 shows that K^+ location at either M(2) or M(4) would totally block either the B or A channel, respectively, leaving only a single channel open for diffusion. One intent of this research is to utilize the diffusion results to elucidate the role of these excess cations. The role of water has been ignored in the above discussion since diffusion studies were carried out using the anhydrous forms of the modified clinoptilolites.

Table 4. Unit Cell Composition of Natural and Modified Clinoptilolites

Element*	TSM-140**	TSM-140	−PUR	$-K^+$	$-Na^+$	$-H^+$	$-Ca^{2+}$	$-Mg^{2+}$
Si	29.54	29.76	29.75	30.05	29.84	29.97	29.78	29.80
Al	5.97	5.67	5.84	5.56	5.68	5.57	5.87	5.88
Fe	0.30	0.34	0.28	0.18	0.20	0.23	0.22	0.22
Ca	1.02	0.62	0.73	0.03	0.02	0.02	2.70	0.44
Mg	0.47	0.44	0.49	0.08	0.08	0.09	0.13	2.20
Na	2.79	3.10	2.93	0.17	5.98	0.16	0.08	0.12
K	1.07	1.37	1.12	5.94	0.33	0.22	0.25	0.45
H_3O	—	—	—	—	—	5.80	—	—
Total No. Ex. Cations	5.35	5.52	5.26	6.22	6.40	6.29	3.16	3.21
Si:Al	4.95	5.25	5.10	5.41	5.25	5.38	5.07	5.07
CEC (meq/g)	2.376	2.109	2.345	2.078	2.025	2.252	2.246	2.259
Extent of Exchange (%)	—	—	—	103.6	101.6	100.0	88.8	72.2

* Elemental concentrations given as no. of atoms/unit cell.
** Based on Steelhead Specialty Minerals data.

Modification by Ion Exchange

Purification and composition analysis

Clinoptilolite (TSM-140) was obtained for this research from Steelhead Specialty Minerals, Spokane, WA. The raw zeolite was crushed to -80 mesh (177 μm), heated in distilled water to remove soluble salts and dispersed in methyl iodide to remove heavy impurities. Approximately 17 wt.% of the original material was removed as impurity. The purified clinoptilolite was employed in all subsequent ion exchanges.

Modified clinoptilolites were analyzed by inductively coupled plasma atomic emission spectroscopy (ICP) using a Thermo Jarrel Ash 61 ICAP instrument to determine the quantities of framework elements and charge-balancing cations. ICP was chosen primarily for its ability to perform accurate multi-element analysis over a wide concentration range on a single sample. Faires (1986) has described the method in detail. Samples were prepared for the ICP analysis using a fusion dissolution technique commonly employed in geochemical analysis (Lichte et al., 1987). Elemental concentrations determined by ICP were translated to unit cell compositions (no. of atoms/unit cell). Compositions of the raw and purified clinoptilolite (PUR) measured in this study are in good agreement with the raw material analysis supplied by Steelhead as shown in Table 4.

Ion exchange

Natural zeolites contain a mixture of elements in the framework, as exchangeable cations and as impurities. Thermodynamic and kinetic ion exchange data are scarce for such multicomponent systems. Since tedious wet chemical and/or single element analytical procedures have been generally relied upon for composition analysis, only a single exchange of the zeolite is typically performed. It is not surprising that the extent of exchange accomplished is often arbitrary. These problems were largely overcome, although not entirely, by employing ICP for composition analysis and applying successive ion exchanges. This insured both complete exchange as well as the removal of any excess salt of the ingoing cation. The importance of reliable composition analysis after ion exchange has been discussed in greater detail by Townsend (1986).

Clinoptilolite, purified as described above, was ground to -100 mesh (149 μm) prior to ion exchange. Exchanges were performed with 1.0N chloride solutions of each of the cations K^+, NH_4^+, Na^+, Ca^{2+}, Mg^{2+} using approximately 10 mL exchange solution/g zeolite. Solution temperatures ranged from 50°C to 121°C. Excess salts of the exchange solutions were found to persist with the zeolite, requiring many repeated washings and subsequent ICP analysis. All modified clinoptilolites were calcined at 100°C after washing and ground to -325 mesh (44 μm) for adsorption studies.

The compositions of the exchange-modified clinoptilolites are compared in Table 4. Since NH_4^+ is not detectable by ICP, full exchange was determined when background levels of Mg^{2+}, Ca^{2+}, K^+, and Na^+ reached a minimum after repeated exchanges. The NH_4^+ clinoptilolite was subsequently analyzed for NH_3 content by the Kjeldahl method. The resulting NH_3 content (0.410 wt.%) represents a NH_4^+ cation fraction of only 10.7%. It is thus concluded that H_3O^+ is the major charge-balancing cation remaining after NH_4^+ exchange and calcination. It is likely that the residual NH_4^+ is converted to H^+ through the release of NH_3 during the activation process (350°C) so that the dehydrated sample used in the diffusion studies is the fully-exchanged H^+ clinoptilolite.

Cation exchange capacity

Although the primary purpose of the ICP measurements is to determine extent of exchange, the quantitative determination of all elements in the structure (except oxygen) provides a convenient means of evaluating the self-consistency of the composition analysis. The Si:Al ratio and cation exchange capacity (*CEC*) can all be computed from the ICP data. For the purpose of charge balance calculations, Fe^{3+} is considered to be located in the framework tetrahedral sites (Roque-Malherbe et al., 1990; Gottardi and Galli, 1985).

The cation exchange capacity can be based on either the amount of $(Al^{3+} + Fe^{3+})$ in the framework or the sum of the equivalent charges provided by the exchangeable cations. The *CEC* has been computed here from the $(Al^{3+} + Fe^{3+})$ sum and is given along with the Si:Al ratio in Table 4. The small variation in the Si:Al ratio over all sorbents is a good measure of the framework integrity after ion exchange. The extent of exchange reported in Table 4 was computed from the ratio of the major cation equivalent charge concentration to the *CEC*. These results confirm the full exchange of the monovalent cations. Additional details of ion exchange and ICP methodology employed in this study have been discussed by Ackley and Yang (1991).

Gravimetric Uptake Measurements

A variety of experimental methods have been used to determine diffusivities of gases and vapors in microporous materials (Karger and Ruthven, 1989). Transport or effective diffusivities can be directly related to gas separations to provide essential information for process modeling, such as pressure swing adsorption (PSA) kinetic separations. Such measurements have also been useful in the present study for analyzing the microscopic effects of channel blockage.

A schematic of the experimental apparatus is shown in Figure 5. The uptake history and equilibrium amount absorbed were determined gravimetrically using a Cahn 2000 System 113 ther-

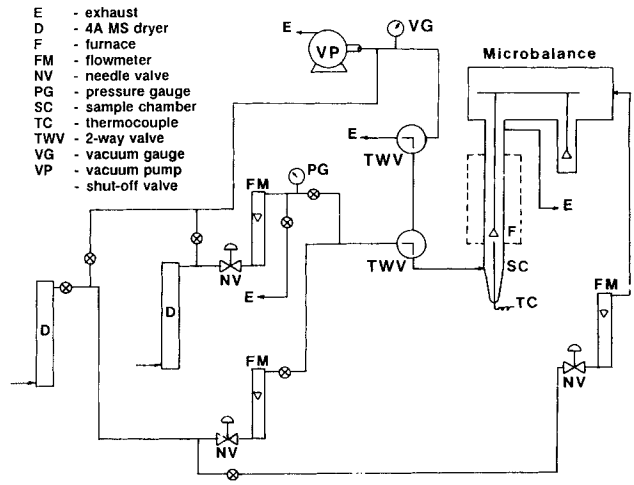

Figure 5. Apparatus used for uptake measurements.

mogravimetric analyzer (TGA). All zeolite samples were regenerated at 350°C for a minimum of 8 h prior to each set of adsorption measurements. Each gas was thoroughly dried by passing through columns containing 500 cm^3 of 4A molecular sieve prior to mixing and introduction to the TGA. A constant pressure, constant flow and constant concentration of a single adsorbate in helium were introduced to the zeolite sample on the electrobalance and maintained until equilibrium was achieved. The total gas flow rate was controlled at 760 cm^3/min, and concentrations were varied by changing the relative flow rates of the adsorbate and helium gases. The adsorbate concentration was determined by gas chromatography. The gravimetric results were corrected for buoyancy and drag effects. A temperature controller maintained the sample chamber at either 27°C or 50°C. Nitrogen (99.99%), methane (99.0%) and helium (99.995%) were purchased from Union Carbide Industrial Gases Inc. A similar method was employed by Yeh (1989).

The structure of clinoptilolite and the properties of the N_2 and CH_4 probe molecules suggest intracrystalline diffusion control. Diffusion time constants (D/L^2) are determined by comparing the uptake data to a diffusion model. The possible effects of concentration dependence of the diffusivity are avoided in this approach by using small differential steps in the gas-phase concentration between successive uptake measurements. Diffusivities are then approximately constant over the small concentration steps but may vary over the entire range of concentration. Uptake measurements for determining intracrystalline diffusivities are subject to possible limitations from external heat and mass transfer resistances, moisture, and hydrodynamic effects. Each of these effects has been addressed below.

Hydrodynamic effects

At the end of each uptake measurement, the flow is diverted from the weighing chamber for a short time to change the adsorbate concentration. When the flow is reintroduced at the new concentration, apparent changes in weight of the sample occur due to the absolute drag force and from variations in both drag and buoyancy forces due to the changes in the gas mixture density and viscosity. The zero-uptake baseline and uptake start time ($t=0$) must be determined accurately. The short-time uptake weight should be large enough, and the gas-phase concentration step small enough, so that the effects of buoyancy and drag changes are minimized.

The 0-100 μg scale of the electrobalance was used for all uptake measurements, and a target short-time uptake of 20 μg was selected for a 20-mg anhydrous zeolite sample. Drag and buoyancy forces were determined using a nonadsorbing blank over the entire concentration range. Changes in buoyancy forces correlated linearly with changes in the mixture density. Actual drag was determined from absolute weight measurements immediately after starting or stopping the flow to the sample chamber. This technique allowed uptakes as small as a few micrograms to be measured.

Moisture

Moisture is a potential interference in measuring the uptake rates of weakly polar gases or vapors on hydrophilic zeolites. The gases used in this study were dried to approximately 0.1 ppm moisture—near the lower limit capability of the 4A molecular sieve at 25°C. Extreme care was taken to eliminate all system leaks. Clean, dry, stainless steel tubing was used for all gas transfer lines leading to the TGA. Moisture adsorption was reduced to approximately 3.0 μg/h for the 20-mg clinoptilolite samples in this study. The adsorption of 10-μg water vapor on a 20-mg sample of clinoptilolite is equivalent to less than 0.06 H_2O molecules/unit cell. Since most adsorption experiments were carried out in less than 10 h, the resulting amount of adsorbed water vapor had minimal effect on the uptake measurements.

Mass transfer limitations

Macropore diffusion limitation, if present in larger particles, should be minimal for the 44-μm particles utilized in the adsorption measurements. The diversity in the crystalline morphology precludes the control of, or even accurate determination of, the crystalline size distribution. As a result, mass and heat transfer limitations must be controlled through the choice of operating conditions.

Mass transfer limitations can result from bulk flow gas diffusion and particle film resistances. Insufficient supply or incomplete mixing of adsorbate gas are to be avoided. All of these effects can be virtually eliminated by providing a sufficiently high flow of gas to the sample. Total flow rates to the TGA were varied from 250 cm^3/min to 1,000 cm^3/min for a constant concentration of N_2 in He. Fractional uptake (M_t/M_∞) was determined at each flow rate for K^+ clinoptilolite as shown in Figure 6. Mass transfer to the sample is limited by one or a combination of the factors described above for flow rates below 760 cm^3/min. Since the bottom of the sample pan faces the incoming flow, it is likely that mixing above the pan near the sample is incomplete (forming a stagnation region) at the lower flow rates. The supply rate of N_2 to the sample chamber at 760 cm^3/min ($y_{N_2}=0.07$) is more than 100 times the highest uptake rate measured. A characteristic time of 0.5 s for diffusion in the bulk flow can be estimated from the binary molecular diffusivities of N_2/He (0.708 cm^2/s) and CH_4/He (0.684 cm^2/s) using the sample pan radius (0.6 cm) as a characteristic dimension. The highest diffusion rates measured for clinoptilolites have characteristic times more than 20 times greater. The effects of external mass transfer limitations are

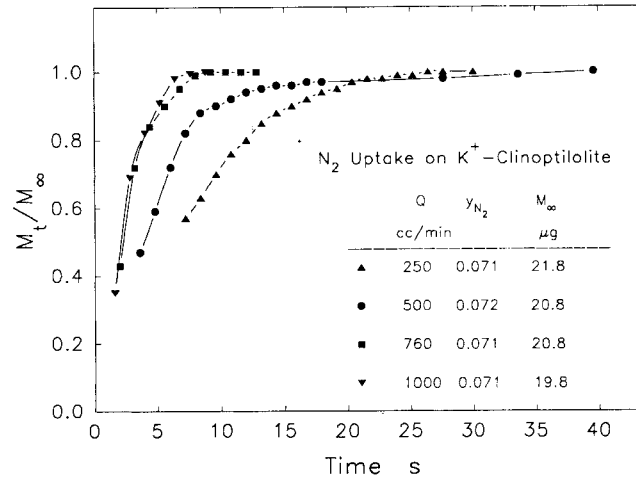

Figure 6. Effect of flow rate on fractional uptake.

thus negligible for the operating conditions chosen. The substantial range of diffusion time constants observed over the various ion-exchanged samples supports intracrystalline diffusion control.

Heat transfer limitations

Of the several possible heat transfer resistances, heat transfer from the sorbent particle or crystal to the surrounding fluid is considered the most limiting. The easiest way to minimize this effect is to maintain near isothermal conditions. Although more extensive treatments are possible (Ruthven et al., 1980), a conservative estimate is sufficient to verify the proper choice of operating conditions.

In this example, the heat of adsorption is assumed to be completely converted to a temperature increase of the zeolite sample. A 20-μg uptake of N_2 by a 20-mg sample of clinoptilolite generates approximately 1.8×10^{-5} kJ [using 25.0 kJ/mol as a nominal value for heat of adsorption (Ackley and Yang, 1991)]. Using a heat capacity of 2.99 kJ/mol·K and a molecular weight of 2,700 g/mol for clinoptilolite (Hemingway and Robie, 1984), the maximum temperature rise of the sample is 0.8 K. The actual temperature rise will be lower due to heat transfer to the surroundings. Thus, the thermal effects on diffusion and adsorption capacity can be neglected under these conditions.

Since the adsorption behavior of the various modified clinoptilolites varied considerably, gas-phase concentration steps were varied as required to insure accuracy and to minimize the limiting factors described above. Self-consistency of the measurements was verified by comparing the overall absolute weight change of the sample with the cumulative weight gain from the differential adsorption steps.

Diffusion Model

Plane sheet model

A diffusion model is required to extract diffusion coefficients from the uptake rate data. Each layer of clinoptilolite channels can be visualized as an independent plane sheet diffusion layer. In the specific case of K^+ clinoptilolite, where all C channels are blocked by K^+ cations, diffusion can occur only along the *c*-axis. A single row of alternating A and B parallel channels then represents a semi-infinite plane through which one-dimensional diffusion occurs. Figure 3 shows a small section of two such diffusion layers.

The 1-D diffusion equation is derived for a semi-infinite plane sheet by applying Fick's law for isotropic media to an overall mass balance of a volume element of the sheet:

$$\frac{\partial q}{\partial t} = D \frac{\partial^2 q}{\partial x^2} \tag{1}$$

Implicit in Eq. 1 are the assumptions of a homogeneous isotropic medium in which D is independent of adsorbate concentration q. An exact form solution of Eq. 1 is given by Crank (1975) for the following plane sheet boundary conditions:

$$q = q_0 \qquad -L < x < L, \qquad t = 0$$

$$q = q_1 \qquad x = -L,\ x = L \qquad t > 0$$

The solution to Eq. 1 is:

$$\frac{q - q_0}{q_1 - q_0} = 1 - \frac{4}{\pi} \sum_{n=0}^{\infty} \frac{(-1)^n}{2n+1} \left[\cos \frac{(2n+1)\pi x}{2L} \right] \exp \left[\frac{-(2n+1)^2 \pi^2 D t}{4L^2} \right] \tag{2}$$

Equation 2 is integrated over the full width ($2L$) of the plane sheet to obtain the fractional uptake relation:

$$\frac{M_t}{M_\infty} = 1 - \frac{8}{\pi^2} \sum_{n=0}^{\infty} \frac{1}{(2n+1)^2} \exp \left[\frac{-(2n+1)^2 \pi^2 D t}{4L^2} \right] \tag{3}$$

M_t/M_∞ in Eq. 3 applies either to a single diffusion layer or to all diffusion layers having equal widths ($2L$) and diffusion coefficients (D). Since M_t/M_∞ represents a volume-averaged adsorbate concentration, it can be determined directly from the measured uptake rate data. The diffusion time constant (D/L^2) averaged over all the crystallites in the sample is determined by fitting Eq. 3 to the measured uptake data (M_t/M_∞) using a Marquardt-Levenberg nonlinear curve fitting algorithm (Press et al., 1989). Excellent agreement with the model was realized for those modified clinoptilolites displaying only a rapid uptake.

Parallel channel model

Many diffusion-controlled processes involve more than a single characteristic diffusion coefficient. Recently, two-component diffusion in zeolite ZSM-5 has been modeled for benzene and toluene (Qureshi and Wei, 1990). The relative contributions of combined pore volume and surface diffusions in porous media have been discussed by Riekert (1985), while Ruckenstein et al. (1971) proposed a bidisperse model for transient diffusion in porous media containing both micropores and macropores. In each of the processes described above, two diffusion coefficients arise due to the presence of more than one diffusion mechanism or more than one diffusing vapor. In the present study, two diffusion time constants appear for entirely different physical reasons due to differences in channel geometry and blockage in the clinoptilolite structure.

Four of the modified clinoptilolites exhibited two distinct uptake regions (rapid and slow) for CH_4. A composite plane sheet composed of independent, eight- and ten-member ring, parallel channels with no interconnections is envisioned using the K^+ clinoptilolite structure. The 1-D diffusion in each of the two types of channels is characterized by a different diffusion time constant:

$$\left(\frac{m_t}{m_\infty} \right)_i = f_i \left(\frac{D_i}{L_i^2} \right) \tag{4}$$

where f_i is the plane sheet 1-D solution of Eq. 3. Applying an overall mass balance to both the transient and equilibrium uptakes results in two additional relationships:

$$M_t = m_{t_1} + m_{t_2} \tag{5}$$

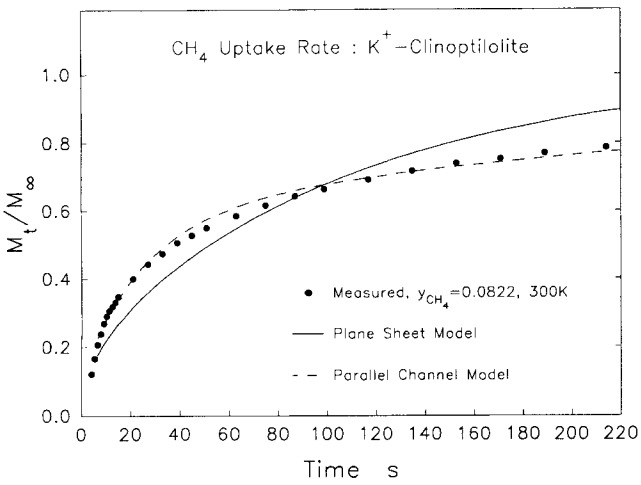

Figure 7. Plane sheet vs. parallel channel models with fractional uptake data for K^+ clinoptilolite.

$$M_\infty = m_{\infty_1} + m_{\infty_2} \tag{6}$$

where m_{t_1}, m_{t_2} and m_{∞_1}, m_{∞_2} are the time-dependent and equilibrium amounts adsorbed, respectively, by each of the two channels. Combining Eqs. 4-6 results in the relationship for the overall uptake rate (the superposition of two independent 1-D processes):

$$\frac{M_t}{M_\infty} = \gamma f_1 + (1-\gamma) f_2 \tag{7}$$

where

$$\gamma = \frac{m_{\infty_1}}{M_\infty} \tag{8}$$

The parameter γ represents the fractional equilibrium amount adsorbed in the channel contributing the rapid diffusion component.

This quasi-isotropic model applies also to diffusion in series in a single channel where the rate-controlling diffusion shifts from an initial rapid uptake into the shallow depths of an unobstructed channel to a hindered diffusion when channel blockages (cations) are encountered. In either case, three unknowns (D_1/L_1^2, D_2/L_2^2, γ) must be determined from the nonlinear fit of the model to the uptake data (M_t/M_∞). The plane sheet (one-parameter) and parallel channel (three-parameter) models are compared with the CH_4 uptake data for K^+ clinoptilolite in Figure 7. Clearly, the CH_4 uptake data are better represented by the parallel channel diffusion model.

Diffusion Characteristics

Diffusion time constants for the six clinoptilolites were determined by applying either the plane sheet or parallel channel diffusion model to the uptake data obtained at 300 K and 323 K. Concentration-dependent diffusion time constants for N_2 and CH_4 are compared for K^+, Mg^{2+}, and H^+ clinoptilolites in Figure 8 and for Na^+, Ca^{2+}, and PUR clinoptilolites in Figure 9. Five of the samples displayed two diffusion coefficients for at least one of the gases. Each component $(D/L^2)_i$ is displayed as a function of the total adsorbate concentration. The equilibrium uptake fraction due to the fast component (m_{∞_1}/M_∞) in the parallel channel model is given in Figure 10.

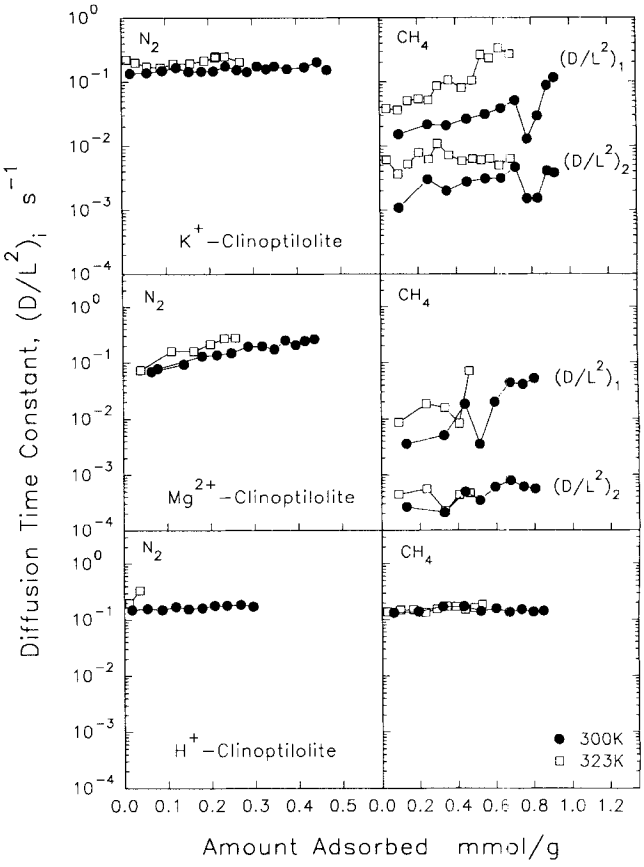

Figure 8. Diffusion time constants for K^+, Mg^{2+} and H^+ clinoptilolites.

Diffusion time constants vary by more than three orders of magnitude (10^{-4} s$^{-1} \le D/L^2 \le 10^{-1}$ s^{-1}) for both N_2 and CH_4 for this group of modified clinoptilolites. Using a nominal characteristic crystal dimension of $L = 1.0$ μm, the corresponding diffusion coefficients vary over the range 10^{-12} cm^2/s $\le D \le 10^{-9}$ cm^2/s.

K^+ and Mg^{2+} clinoptilolites

These two modified clinoptilolites provide the best physical representations of 1-D plane sheet diffusion for N_2 and 1-D parallel channel diffusion for CH_4. The single-component, concentration-independent diffusion of N_2 in K^+ clinoptilolite shown in Figure 8 is consistent with either of the following:

1. Single channel diffusion (A or B with the other channel completely blocked)

2. Diffusion in both parallel channels A and B with $D_A = D_B$.

Parallel channel diffusion is clearly evident for CH_4 in both Figures 7 and 8 for the K^+ zeolite. The fast component $(D/L^2)_1$ for CH_4 diffusion increases with adsorbate concentration, while the slower component $(D/L^2)_2$ is approximately constant. The CH_4 adsorbate equilibrium concentration is divided almost equally between the two components as shown in Figure 10.

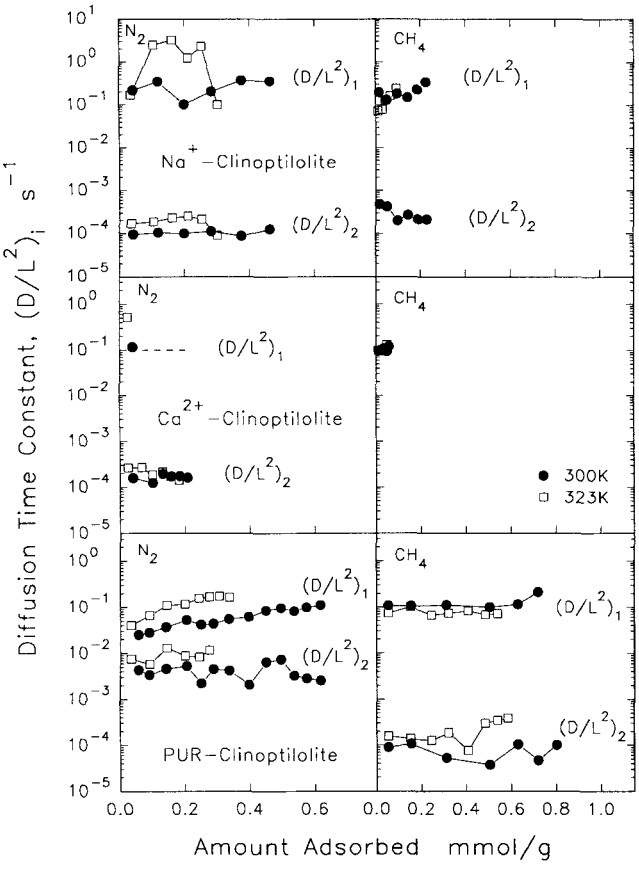

Figure 9. Diffusion time constants for Na^+, Ca^{2+} and PUR clinoptilolites.

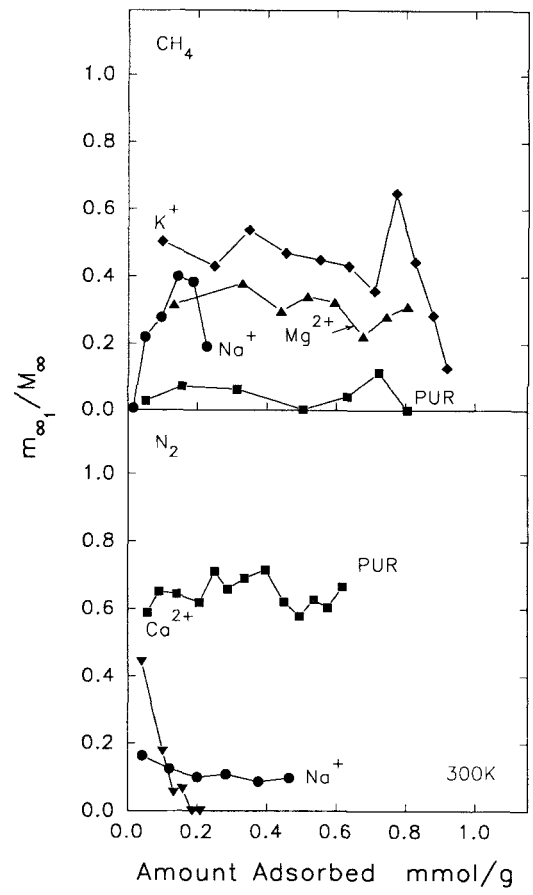

Figure 10. Equilibrium fraction in modified clinoptilolites with both rapid and slow diffusion components.

Recalling the discussion above concerning the location of the two excess K^+ cations, the diffusion data indicate that occupancy of either M(2) or M(4) is highly unlikely. This conclusion is further supported by the pore volume calculations of Ackley and Yang (1991) showing no pore volume reduction (molecular sieving) of either CH_4 or N_2 for K^+ clinoptilolite—a necessary condition if either M(2) or M(4) were occupied by K^+ in conjunction with the saturation of M(3). An explanation consistent with both the adsorption and diffusion characteristics is the twofold coordination of K^+ cations about alternating M(3) sites: two K^+ cations locate on each side of the eight-member ring and cause a partial blockage of both the A and B channels. The remaining half of the M(3) sites would contain only a single K^+ cation at the center of the eight-member ring.

Full exchange of the Mg^{2+} cation was not achieved and the channel blockage given in Table 3 must be modified to account for the other cations present. The M(4) site is saturated with Mg^{2+} according to the ICP results in Table 4. Ca^{2+} and K^+ cations, in approximately equal numbers, account for the majority of the remaining charge balance. Since the M(1)-M(4) combination is a forbidden pair of sites (Koyama and Takeuchi, 1977) Ca^{2+} is most likely to be found at the M(2) site, while the K^+ cation will locate at the M(3) site. The Ca^{2+} in the M(2) site results in significant blockage of the B channels. Coupled with the complete blockage of A channels by the Mg^{2+} cation, the resulting diffusion path is primarily 1-D along the *a* axis through the C channels. As illustrated in Figure 4c, occupancy of the M(2) site gives rise to partial blockage of the C channel. Since this site is not saturated, parallel channel diffusion (with two diffusion coefficients) is quite likely since a combination of unblocked channels, complete blockage [K^+-M(3)] and partial blockage [Ca^{2+}-M(2)] conditions exist for the C channel. The CH_4 results for Mg^{2+} clinoptilolite in Figure 8 reveal the two diffusion coefficients expected. Both components of diffusion for the Mg^{2+} sample are smaller than those for K^+ clinoptilolite consistent with the difference between ten-member and eight-member ring diffusion for $(D/L^2)_1$ and the smaller size of the eight-member ring of the C channel compared to that of the B channel with respect to $(D/L^2)_2$. The rapid component of CH_4 diffusion $(D/L^2)_1$ accounts for about one-third of the equilibrium uptake as shown in Figure 10. The N_2 diffusion time constant is comparable in magnitude to that for the K^+ clinoptilolite but clearly increases with adsorbate concentration. This concentration dependence may be the result of the N_2 quadrupole interaction with the Mg^{2+} cation revealed by the energetic heterogeneity determined from isosteric heats of adsorption (Ackley and Yang, 1991).

H^+ clinoptilolite

The location of the H^+ cation in the clinoptilolite structure is unknown, but a previous adsorption study shows this form of clinoptilolite to have a very open structure (Barrer and Makki, 1964). The results in Figure 8 confirm an open channel

system and are consistent with the complete conversion of the NH_4^+ cation as suggested above. The plane sheet diffusion behaviors of N_2 and CH_4 are almost identical, showing equal magnitude of diffusion time constant and no concentration dependency.

Na^+, Ca^{2+} and PUR clinoptilolite

These modified clinoptilolites present a more complex structure for which the simple parallel channel system can no longer be rationalized. Slow and rapid diffusion, however, is clearly evident in the uptake data for these materials, and the parallel channel model remains a useful tool to investigate the diffusion behavior and structure of these materials. The resulting effective diffusion time constants are compared on the same basis for nitrogen, methane, and the various modified clinoptilolites.

Molecular sieving of N_2 and CH_4 in Na^+ clinoptilolite has been demonstrated through pore volume approximations (Ackley and Yang, 1991). The uptake is generally split between the rapid and slow diffusion components. These factors result in greatly reduced uptake amounts for these gas-zeolite combinations, making the gravimetric measurements more difficult.

The diffusion results for Na^+ clinoptilolite are given in Figure 9. The slow diffusion component $(D/L^2)_2$ is dominant for both N_2 and CH_4 as evidenced by the relatively low values of m_{∞_1}/M_∞ shown in Figure 10. The diffusion time constants for N_2 and CH_4 are nearly the same. The variation in $(D/L^2)_1$ at 323 K is due primarily to the small but rapid uptake (only a few uptake readings are possible) and the stiffness of the nonlinear curve-fitting method. These factors, however, have very little influence on determining $(D/L^2)_2$. It is apparent from Figure 4 that restricted diffusion occurs primarily in the A and C channels, while the B channel is completely blocked. Because of the small fraction of the total uptake due to $(D/L^2)_1$, the C channel is probably further restricted by the two excess cations. The disappearance of $(D/L^2)_2$ for CH_4 at 323 K is consistent with the possible migration of Na^+ cations at elevated temperature (Ackley and Yang, 1991).

The Ca^{2+} clinoptilolite diffusion results are somewhat surprising in view of the smaller number of cations present. The slow component of CH_4 diffusion disappears completely, and the sieving of both N_2 and CH_4 is evident by the reduced adsorption amounts. The small amount of Mg^{2+} present (5–10%) appears to have a significant effect on diffusion. If Mg^{2+} locates near the crystal surface at M(4) sites, then the A channels can be completely blocked by only few Mg^{2+} cations. Another possible factor is the increased blockage of the C channels when the M(2)′ site is occupied. The rapid component of diffusion saturates at low N_2 adsorbate concentration on the Ca^{2+} zeolite as evidenced by the sharp decline in (m_{∞_1}/M_∞) in Figure 10. This result further supports the dead-end channel concept. Comparing the Ca^{2+} and Mg^{2+} clinoptilolite diffusion results emphasizes the great efficiency at which the Ca^{2+} cation blocks the eight-member ring channels.

PUR clinoptilolite contains four exchangeable cations (56% Na^+, 21% K^+, 14% Ca^{2+}, 9% Mg^{2+}). The 5.26 cations per unit cell given in Table 4 represents a reduction in excess cations from the fully-exchanged monovalent zeolites. An interesting kinetic selectively exists in this sample as shown by the results in Figure 10. Approximately 60% of the N_2 enters through the rapid diffusion component, while 95% of the CH_4 enters through the slow component. This "transient molecular sieving" is likely due to the effective blocking of the A channels by Mg^{2+} and Ca^{2+} cations and less restriction to N_2 diffusion from fewer excess cations.

The relatively low concentration dependence of D/L^2 for most of the cases in this study reflect the low sorbate concentrations of N_2 and CH_4; for example, at the highest capacities measured, the concentration of N_2 or CH_4 approaches only 1.0 to 2.0 molecules/unit cell. Diffusion time constants increase for several samples, however, and these increases are well above the experimental uncertainty in the uptake rate measurements. The unblocked eight- and ten-member rings provide only moderate restriction to CH_4 and N_2 diffusion. Restricted diffusion is pronounced in all channels blocked by cations, and differentiation between CH_4 and N_2 is mainly the result of shape selectivity. Molecular sieving occurs when channel openings become completely blocked in such a manner that channel regions become inaccessible to sorbate molecules.

Equilibrium capacity

Equilibrium coverage is also affected by cation charge and number for the weakly polar N_2 molecule (Ackley and Yang, 1991). These effects are less pronounced for the nonpolar CH_4 molecule. Molecular sieving, when it occurs, has the most significant effect on capacity due to the reduction of accessible pore volume. In such cases, the cation location becomes the dominant factor. The highest amounts adsorbed shown in Figures 8 and 9 reflect the equilibrium capacity at a pressure of approximately 1.0 atm. The lowest N_2 capacity at 1.0 atm occurs for Ca^{2+} clinoptilolite due to molecular sieving. The second lowest N_2 capacity occurs for H^+ clinoptilolite due to the low interaction energy as evidenced by the smallest values of the isosteric heat of adsorption.

Activation energy

The temperature dependence of diffusivity is often described:

$$D = D_0 \exp[-E_A/RT] \tag{9}$$

where E_A is the energy of activation of the diffusion process and D_0 is the diffusivity at zero adsorbate concentration. E_A can be computed for both the rapid and slow components of diffusion. The N_2 diffusion data in this study show very little temperature dependence over the narrow range 300 K–323 K. For the rapid diffusion component, this result is consistent with relatively unrestricted diffusion accompanied by low activation energy.

Activation energies can only be approximated from the data in Figures 8 and 9. The accuracy of such approximations are limited by the fact that diffusion was determined at only two closely-spaced temperatures. Those cases showing a decrease in D/L^2 with temperature may be associated with cation migration—a condition that effectively changes the structure and makes any associated activation energy meaningless. Overall, activation energy determination is limited by the lower adsorption capacities at moderately elevated temperatures and

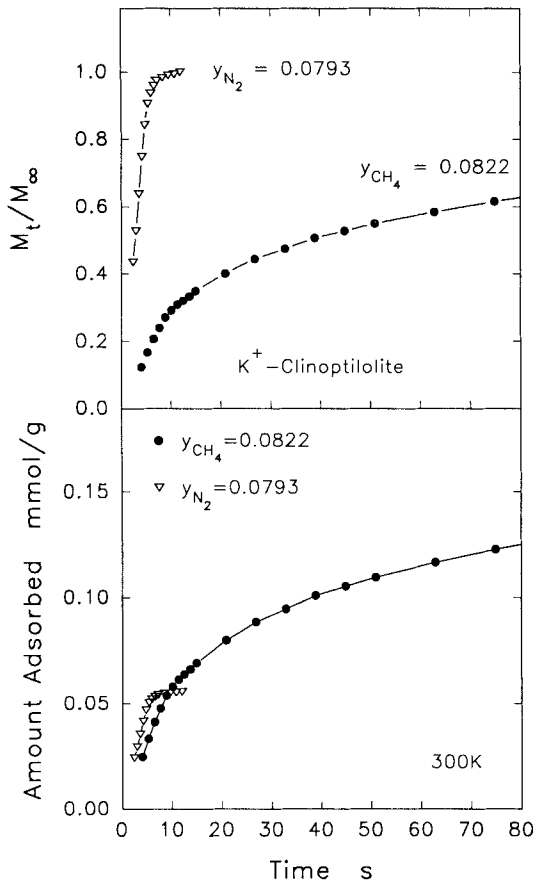

Figure 11. Fractional vs. mole uptake rates for K^+ clinoptilolite.

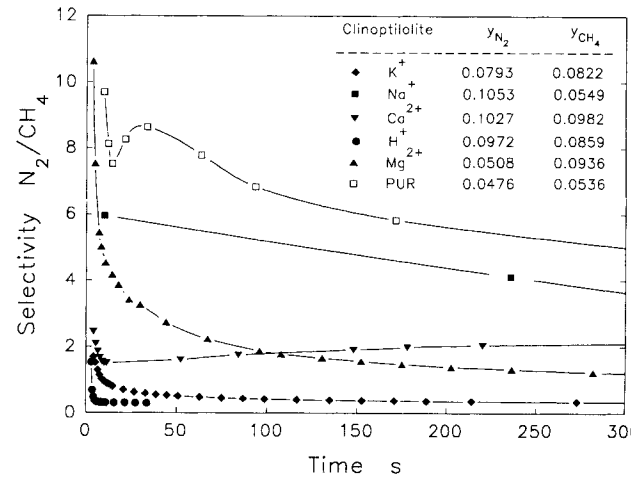

Figure 12. Kinetic selectively of modified clinoptilolites based on uptake on clean surface ($q=0$).

the very low uptake rates that would result at subambient temperatures.

Kinetic Separation

The difference in kinetic behavior of two adsorbing gases can be exploited by PSA processes in bulk gas separations to concentrate the desired product (Yang, 1987). The separation of N_2/CH_4 mixtures based on the difference in the diffusion rates of these gases into the sorbent is very difficult due to the small difference in the kinetic diameters of the gas molecules. Furthermore, certain PSA process advantages are not available when the desired product (CH_4) is also the more strongly adsorbed component—the usual case for CH_4/N_2 mixtures with most sorbents. For the modified clinoptilolites of this study, Ackley and Yang (1991) have shown that N_2 is preferentially adsorbed at equilibrium only in the Ca^{2+} and Na^+ materials where molecular sieving of CH_4 has been affected. These factors make kinetic separation of N_2/CH_4 mixtures potentially more attractive than equilibrium separation.

Habgood (1958b) expressed the separation factor as the product of the equilibrium selectivity and the square root of the diffusivity ratio. This definition provides a reasonable estimate of the true separation factor when $M_t/M_\infty \propto \sqrt{t}$. Kinetic selectivity, however, is often evaluated by comparing the uptake histories (M_t/M_∞ vs. t) or calculated as the ratio of the diffusion coefficients in binary systems. Such comparisons can be misleading when the molecular weights and M_∞ values differ significantly for the two gases as illustrated in Figure 11. For example, comparing uptake rates (M_t/M_∞) for CH_4 and N_2 ($q=0$ at $t=0$) for K^+ clinoptilolite indicates a high initial N_2 selectivity, as does the ratio of diffusion time constants, $[D(N_2)/L^2]_1/[D(CH_4)/L^2]_1 \approx 10$. The true kinetic selectivity is determined only when the mole uptake rates of the two gases are directly compared as shown in the bottom portion of Figure 11. It is evident that there is no short-term kinetic selectivity of either gas, while only CH_4 is adsorbed beyond 10 s.

True kinetic selectivity or initial separation factor is time-dependent. Kinetic selectivity has been determined for the modified clinoptilolites as the ratio of the N_2/CH_4 mole uptake rates, as shown in Figure 12. The results in Figure 12 were obtained from the initial uptakes on a completely desorbed sample ($q=0$ at $t=0$). The gas-phase concentrations of N_2 and CH_4 for the adsorption step are indicated in the figure. The time period for an adsorption step in a PSA cycle is typically in the range of 30–300 s, and a N_2/CH_4 selectivity > 1.0 is desirable for this separation. The selectivities in Figure 12 approach the equilibrium separation factor at sufficiently long times. The kinetic separation factors vary by almost two orders of magnitude for this group of sorbents, but favorable N_2 selectivity occurs for several of these materials in a time range (0–10 s) that is not practical for commercial PSA cycles.

Interestingly, the purified natural clinoptilolite has the largest kinetic selectivity sustained over the longest time period. This is the result of the transient molecular sieving described above where the diffusivity ratio is nearly 1,000. This diffusivity ratio is identical to that reported by Frankiewicz and Donnelly (1983) for a partially Ca^{2+}-exchanged natural clinoptilolite. The true separation factor as shown in Figure 12, however, is less than 10.

Conclusions

Clinoptilolite has been modified by ion exchange to produce a group of sorbents with diffusion characteristics that span more than three orders of magnitude with respect to adsorption of nitrogen and methane. This diffusion behavior has been related to the type, location and distribution of cations in the

clinoptilolite structure through plane sheet and parallel channel diffusion models. Ca^{2+} and Na^{+} cations have been shown to block eight-member ring channels very effectively, while Mg^{2+} completely blocks the ten-member ring channel. Cation location is far more important to channel blocking than size or number. Using the results of this study, it should now be possible to manipulate the clinoptilolite structure further through the selected combination of cations to optimize the difficult separation of CH_4 and N_2, as well as other specific gas mixtures, by kinetic means.

Acknowledgment

This work was supported by NSF Grant CTS 8914754.

Notation

a,b,c = unit cell coordinate axes, unit cell dimensions, nm
CEC = cation exchange capacity, meq/g
D = diffusion coefficient, cm^2/s
D_0 = diffusion coefficient at $q=0$, cm^2/s
D/L^2 = diffusion time constant, s^{-1}
E_A = activation energy of diffusion, kJ/mol
L = half-width of plane sheet, cm
M = amount of gas adsorbed, mmol or g
m = amount of gas adsorbed through rapid (1) or slow (2) diffusion
n = integer
q = adsorbate concentration, $mmol/cm^3$ solid or mmol/g solid
R = gas constant, $R=8.314$ J/mol·K
t = time, s
T = temperature, K or °C
v_∞ = velocity of gas in TGA sample chamber, cm/s
x = distance along diffusion path in plane sheet
y = gas-phase mole fraction

Greek letters

β = angle between a and c coordinate axes of unit cell, rad
γ = fractional amount adsorbed at equilibrium due to the fast component of diffusion
μ = viscosity, g/cm·s

Subscripts

∞ = equilibrium conditions
t = conditions at time t

Literature Cited

Ackley, M. W., "Separation of Nitrogen and Methane by Adsorption: I. Pressure Swing Adsorption Modeling; II. Adsorption and Diffusion in Ion-Exchanged Clinoptilolites," PhD Diss., State Univ. of New York at Buffalo (1991).
Ackley, M. W., R. F. Giese, and R. T. Yang, "Clinoptilolite: Untapped Potential for Gas Separations," *Zeolites*, submitted (1991).
Ackley, M. W., and R. T. Yang, "Adsorption Characteristics of High-Exchange Clinoptilolites," *Ind. Eng. Chem. Res.*, accepted (1991).
Ackley, M. W., and R. T. Yang, "Kinetic Separation by Pressure Swing Adsorption: Method of Characteristics Model," *AIChE J.*, **36**, 1229 (1990).
Alberti, A., "The Crystal Structure of Two Clinoptilolites," *Tschermaks Min. Petr. Mitt.*, **22**, 25 (1975).
Barrer, R. M., *Hydrothermal Chemistry of Zeolites*, Academic Press, London (1982).
Barrer, R. M., and M. B. Makki, "Molecular Sieve Sorbents from Clinoptilolite," *Can. J. Chem.*, **42**, 1481 (1964).
Barrer, R. M., R. Papadopoulos, and L. V. C. Rees, "Exchange of Sodium in Clinoptilolite by Organic Cations," *J. Inorg. Nucl. Chem.*, **29**, 2047 (1967).
Breck, D. W., *Zeolite Molecular Sieves*, Wiley, New York (1974).
Chi, C.-H., and L. B. Sand, "Synthesis of Na- and K- Clinoptilolite Endmembers," *Nat.*, **304**, 255 (1983).
Crank, J., *The Mathematics of Diffusion*, Claredon Press, Oxford (1975).
Faires, L. M., "Inductively Coupled Plasma Atomic Emission Spectroscopy," *Metals Handbook*, 9th ed., V10 Materials Characterization, ASM, Metals Park, OH (1986).
Frankiewicz, T. C., and R. G. Donnelly, "Methane/Nitrogen Gas Separation over the Zeolite Clinoptilolite by the Selective Adsorption of Nitrogen," *Industrial Gas Separations*, T. E. Whyte, Jr., et al., eds., ACS, Washington, DC (1983).
Goto, Y., "Synthesis of Clinoptilolite," *Amer. Mineral.*, **62**, 330 (1977).
Gottardi, G., and E. Galli, *Natural Zeolites*, Springer-Verlag, Berlin (1985).
Habgood, H. W., "Removal of Nitrogen from Natural Gas," U.S. Patent 2,843,219 (1958a).
Habgood, H. W., "The Kinetics of Molecular Sieve Action: Sorption of Nitrogen-Methane Mixtures by Linde Molecular Sieve 4A," *Can. J. Chem.*, **36**, 1384 (1958b).
Hemingway, B. S., and R. A. Robie, "Thermodynamic Properties of Zeolites: Low-Temperature Heat Capacities and Thermodynamic Functions for Phillipsite and Clinoptilolite: Estimates of the Thermochemical Properties of Zeolitic Water at Low Temperature," *Amer. Mineral.*, **69**, 692 (1984).
Karger, J., and D. M. Ruthven, "On the Comparison Between Macroscopic and NMR Measurements of Intracrystalline Diffusion in Zeolites," *Zeolites*, **9**, 267 (1989).
Koyama, K., and Y. Takeuchi, "Clinoptilolite: The Distribution of Potassium Atoms and its Role in Thermal Stability," *Z. Kristallogr.*, **145**, 216 (1977).
Lichte, R. E., D. W. Golightly, and P. J. Lamothe, "Inductively Coupled Plasma-Atomic Emission Spectrometry," *Methods for Geochemical Analysis*, P. A. Baedecker, ed., U.S. Geol. Survey Bulletin 1770, USGPO, Washington, DC (1987).
Ma, Y. H., and T. Y. Lee, "Sorption and Diffusion Properties of Natural Zeolites," *Natural Zeolites*, L. B. Sand and F. A. Mumpton, eds., Pergamon Press, Oxford (1978).
Merkle, A. B., and M. Slaughter, "Determination and Refinement of the Structure of Heulandite," *Amer. Mineral*, **53**, 1120 (1968).
Mumpton, F. A., and W. C. Ormsby, "Morphology of Zeolites in Sedimentary Rocks by Scanning Electron Microscopy," *Clays Clay Miner.*, **24**, 1 (1976).
Nightengale, E. R., "Phenomenological Theory of Ion Solvation: Effective Radii of Hydrated Ions," *J. Phys. Chem.*, **63**, 1381 (1959).
Press, W. H., B. P. Flannery, S. A. Teukolsky, and W. T. Vetterling, *Numerical Recipes*, Cambridge Univ. Press, New York (1989).
Qureshi, W. R., and J. Wei, "One- and Two-Component Diffusion in Zeolite ZSM-5 I. Theoretical," *J. Catal.*, **126**, 126 (1990).
Qureshi, W. R., and J. Wei, "One- and Two-Component Diffusion in Zeolite ZSM-5 II. Experimental," *J. Catal.*, **126**, 147 (1990).
Riekert, L., "The Relative Contribution of Pore Volume Diffusion and Surface Diffusion to Mass Transfer in Capillaries and Porous Media," *AIChE J.*, **31**, 863 (1985).
Roque-Malherbe, R., C. Díaz-Aguila, E. Reguera-Ruíz, J. Fundora-Lliteras, L. López-Colado, and M. Hernández-Vélez, "The State of Iron in Natural Zeolites: A Mossbauer Study," *Zeolites*, **10**, 685 (1990).
Ruckenstein, E., A. S. Vaidyanathan, and G. R. Youngquist, "Sorption by Solids with Bidisperse Pore Structures," *Chem. Eng. Sci.*, **26**, 1305 (1971).
Ruthven, D. M., L.-K. Lee, and H. Yucel, "Kinetics of Nonisothermal Sorption in Molecular Sieve Crystals," *AIChE J.*, **26**, 16 (1980).
Torii, K., M. Hotta, and M. Asaka, "Adsorption Properties of Cation Exchanged Clinoptilolite $(I)^+$," *Nendo Kagaku*, **15**, 23 (1975).
Townsend, R. P., "Ion Exchange in Zeolites: Some Recent Developments in Theory and Practice," *Proc. Int. Zeolite Conf.*, Y. Murakami, et al., eds., Kodansha-Elsevier, Tokyo (1986).
Yang, R. T., *Gas Separation by Adsorption Processes*, Butterworths, Boston (1987).
Yeh, Y.-T., "Diffusion and Adsorption of Gases in Molecular Sieves," PhD Diss., State Univ. of New York at Buffalo (1989).

Manuscript received July 22, 1991, and revision received Sept. 16, 1991.